Journal of Power Sources 199 (2012) 138–141

Contents lists available at SciVerse ScienceDirect

Journal of Power Sources

journal homepage: www.elsevier.com/locate/jpowsour

Short communication

Enabling catalysis of Ru–CeO_2 for propane oxidation in low temperature solid oxide fuel cells

Xuejiao Liu, Zhongliang Zhan*, Xie Meng, Wenhua Huang, Shaorong Wang, Tinglian Wen

CAS Key Laboratory of Materials for Energy Conversion, Shanghai Institute of Ceramics, Chinese Academy of Sciences (SICCAS), 1295 Dingxi Road, Shanghai 200050, China

ARTICLE INFO

Article history:
Received 3 July 2011
Received in revised form
21 September 2011
Accepted 22 September 2011
Available online 13 October 2011

Keywords:
Low temperature solid oxide fuel cells
Catalyst
Partial oxidation
Propane
Hydrocarbons

ABSTRACT

This paper reports on integration of a supported thin film catalyst as a reformer, consisting of nano-scale ruthenium particles well dispersed in the ceria matrix, into the anode chamber of a ceria-electrolyte solid oxide fuel cells (SOFCs). Operation on the propane–air fuel mixture yields maximum power densities of 395 mW cm^{-2}, 280 mW cm^{-2} and 160 mW cm^{-2} at 500, 450 and 400 °C, respectively. In comparison, the output power densities drop to 298 mW cm^{-2} at 500 °C and <10 mW cm^{-2} at 450 °C in the absence of the catalyst layer. The substantially enhanced performance can be explained by the high catalytic activity of the Ru–CeO_2 layer for propane partial oxidation reactions, producing higher amount of hydrogen available for the fuel cell operation and thereby reducing the anodic polarization resistance.

1. Introduction

The solid oxide fuel cell (SOFC) is an electrochemical device for energetically efficient and environmentally clean conversion of fuels into electricity. The present state-of-the-art SOFCs consist of thin yttrium-stabilized zirconia (YSZ) electrolytes supported on Ni–YSZ anode substrates, and usually operate at temperatures $T \geq 700$ °C [1]. Compared with low temperature polymer-electrolyte-membrane (PEM) fuel cells, SOFCs display distinctive features including high temperature operation, high energy efficiency as well as great adaptability to varieties of hydrocarbon fuels. However, direct use of hydrocarbon fuels in SOFCs usually result in the anode deactivation due to coking formation at elevated temperatures, especially for nickel cermet anodes [2]. While significant advances have been made in alternative anode materials that are resistant to coking and show promise for stable operation with hydrocarbon fuels, they are usually less electrochemically active than nickel cermet anodes and thus typically produce substantially lower power densities [3–7]. An effective approach utilizing the nickel cermet anodes for hydrocarbon fueled SOFCs is to internally reform hydrocarbons [8–11]. As an example, internal partial oxidation of propane has been demonstrated in thin YSZ-electrolyte SOFCs, yielding power densities of 700 mW cm^{-2} at 790 °C and 380 mW cm^{-2} at 690 °C [8].

Reduction in the SOFC operating temperature down to 400–600 °C has been actively undertaken due to additional important advantages such as reduced materials cost, improved component durability and easier gas sealing. Anode-supported SOFCs with thin electrolytes of doped ceria have shown great promise for maintaining high power densities at such low temperatures, *e.g.*, 1000 mW cm^{-2} and 400 mW cm^{-2} when operated on humidified hydrogen at 600 °C and 500 °C [12,13], respectively. In the meanwhile, hydrocarbon reforming reactions become increasingly difficult with decreasing temperatures, thereby limiting power output for internal reforming low-temperature SOFCs, especially for $T < 500$ °C [14]. Taking internal methane reforming SOFCs as an example, the power output could be as high as 350 mW cm^{-2} at 550 °C, but became negligibly small at 450 °C. Upon integration of a CeO_2 catalyst layer on the anode surface, the power density at 450 °C increased rapidly to 110 mW cm^{-2} [14]. Hibino et al. reported internal partial oxidation of propane in single-chamber SOFCs, yielding power densities of 240 mW cm^{-2} at 550 °C [15]. Prior report showed that the Ru–CeO_2 catalyst layer can catalyze propane partial oxidation at temperatures down to 400 °C [9]. Coating of such a Ru–CeO_2 catalyst layer on the nickel anode surface allowed thermally self-sustaining operation of single-chamber SOFCs in propane–air fuel mixtures, yielding maximum power densities of ≈240 mW cm^{-2} at 550 °C [16]. Nonetheless, high space velocity, as required to prevent fuel turbulence between the electrodes and thus achieve high power densities, substantially reduces the fuel utilization and thereby the efficiency. The present work was undertaken with the aim of developing high power density

* Corresponding author. Tel.: +86 21 6998 7669; fax: +86 21 6998 7669.
E-mail addresses: zzhan@mail.sic.ac.cn, zhongliangzhan@gmail.com (Z. Zhan).

0378-7753/$ – see front matter © 2011 Elsevier B.V. All rights reserved.
doi:10.1016/j.jpowsour.2011.09.072

low-temperature SOFCs operating on propane for portable and transportation applications such as small power generators or auxiliary power units. To enable efficient propane oxidation at reduced temperatures, a separate Ru–CeO_2 catalyst layer supported on a porous ceramic disc was integrated adjacent to the nickel cermet anode.

2. Experimental

The low-temperature SOFCs were fabricated using the standard ceramic processing procedure as described elsewhere [17]. Anode powders of NiO and SDC in a weight ratio of 60:40 were ball-milled for 20 h with ethanol as the medium, then 10% starch was added and ball-milled for 4 h. The powders were dried at 80 °C, screened with a 120-mesh sieve and pressed into pellets. After firing at 800 °C for 4 h, 12-μm thick NiO–SDC anode active layers and 6-μm thick thin SDC electrolyte layers were colloidally coated on the NiO–SDC supports. The supports and the deposited layers were then co-fired at 1350 °C for 4 h to densify the electrolyte thin films. Cathode active layers consisted of $La_{0.6}Sr_{0.4}Co_{0.2}Fe_{0.8}O_3$ (LSCF) mixed with 30 wt.% SDC, fired at 1100 °C for 4 h. A second current collecting layer of pure LSCF was then applied and fired at 1100 °C for 4 h. The diameter of the final fuel cells was ≈1.4 cm with a thickness of 0.6 mm. The porosity of the anode support was approximately 35% before reduction.

The catalyst was prepared on porous discs consisting of partially stabilized zirconia (PSZ) and CeO_2, chosen primarily because they are inert to coking formation in hydrocarbon fuels. PSZ and CeO_2 powders in a weight ratio of 50:50 were ball-milled with starch filler to introduce a substantial porosity, pressed into pellets of ≈0.3 mm thick, and fired at 1400 °C for 6 h, after which they had a porosity of ≈45%. RuO_2 and CeO_2 powders in a weight ratio of 1:10 were combined in a colloidal suspension with ethanol as the solvent, deposited on both sides of the PSZ–CeO_2, and fired at 900 °C for 4 h to form thin catalyst layers. The microstructure of the catalyst layers was examined using SEM (JSM6390LV, JEOL).

Single SOFCs were tested using a four-probe method in a tube furnace at temperatures from 350 °C to 600 °C. The anode sides of the cells were sealed to alumina tubes using a silver paste. Ag current collectors were painted in grids on the anode and cathode surfaces. In many cases the PSZ–CeO_2 supported Ru–CeO_2 catalysts were positioned directly against the SOFC anodes. Since the thick insulating catalyst layer prevented current collection through the anode surface, current was collected at the side of the anode, as previously illustrated [17]. Ambient air was maintained on the cathode side. At the start of each test, humidified hydrogen was flowed through the anode compartment with the cell at ≈500 °C for ≈12 h, by which time the anode was reduced to Ni–SDC. After baseline testing in humidified hydrogen, test was done in a fuel mixture of 10.7% propane–89.3% air which showed negligible kinetic tendency for coking formation at elevated temperatures even though coking was thermodynamically favourable [8]. *I–V* curves and electrochemical impedance spectra (EIS) were obtained using an IM6 Electrochemical Workstation (ZAHNER, Germany). The frequency range for impedance measurement was 0.1 Hz–100 kHz.

3. Results and discussion

Shown in Fig. 1a is the fracture cross-sectional SEM micrograph of a typical catalyst layer after the fuel cell testing. RuO_2 was in situ reduced to metallic Ru when exposed to hydrogen, as confirmed by X-ray diffraction patterns before and after fuel cell testing. The PSZ–CeO_2 support exhibited a high porosity of ≈45% with pore sizes typically between 2 and 10 μm, as designed to reduce gas transport resistance. The Ru–CeO_2 catalyst layer was ≈30 μm thick

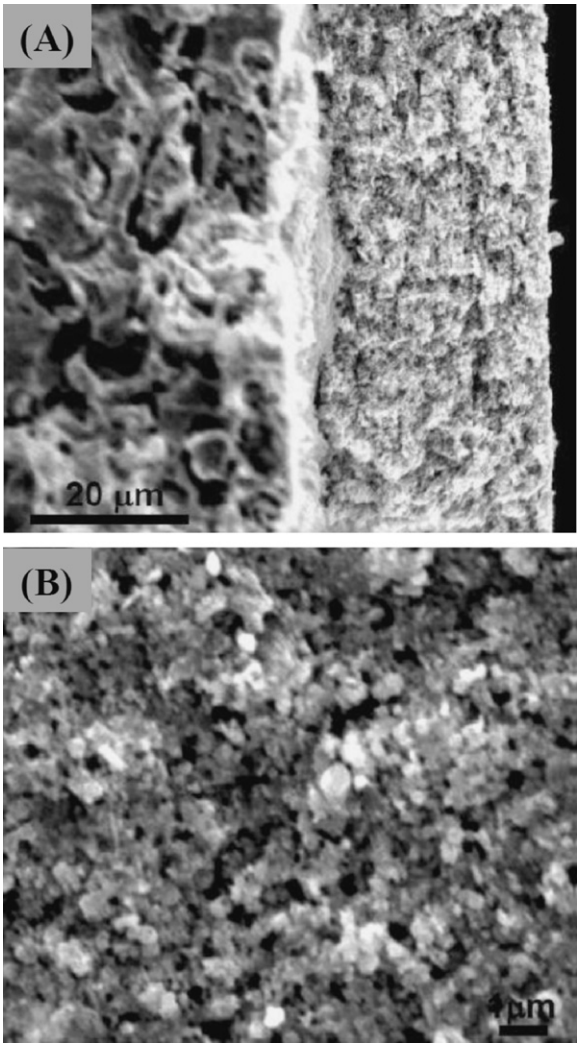

Fig. 1. SEM microstructure of the Ru–CeO_2 catalyst layer supported on the porous PSZ–CeO_2 substrate taken after fuel cell testing: (a) fracture cross-sectional image and (b) surface image.

with an estimated porosity of 30%. Note that firing the catalyst layer at 900 °C yielded a much finer microstructure than for the PSZ–CeO_2 support fired at 1400 °C. Fig. 1b, a higher magnification surface SEM image of the catalyst layer, showed that Ru particles were homogeneously dispersed in the porous CeO_2 matrix, where the distinct white, gray and black region corresponded to the Ru, CeO_2, and pore phases, respectively. The average particle size for Ru was approximately 350 nm, and the mean pore size was around 300 nm.

Prior reports have shown that the Ru–CeO_2 catalyst layer can provide stable catalytic activity for hydrocarbon reforming reactions to maintain stable fuel cell operation [9,16–18]. Typical polarization curves of the voltage *V* and power density *P* vs. current density *J* obtained at 500 °C from two types of fuel cells, one integrated with an adjacent Ru–CeO_2 catalyst layer as a fuel reformer and one without, are shown in Fig. 2a. Comparison of the *J–V* curves suggests that the thin Ru–CeO_2 catalyst layer is highly effective in enhancing the fuel cell performance. In particular, the fuel cell integrated with a Ru–CeO_2 catalyst layer delivered a maximum power density of 395 mW cm^{-2}, while, in the absence of a catalyst layer, the maximum power density dropped by 25% down to 298 mW cm^{-2}. Note that the open circuit voltage (V_{OC}) values, ≈0.87 V for both types of fuel cells, were substantially lower than the thermodynamically value of 1.0 V [9], which is usually ascribed

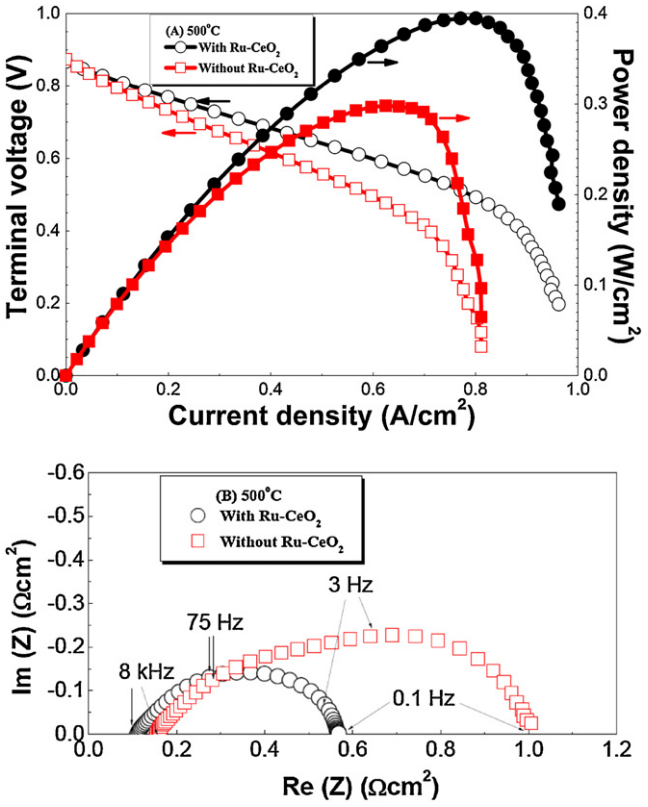

Fig. 2. Comparison of (a) voltage and power density vs. current density curves and (b) Nyqusit plots of electrochemical impedance spectroscopy for the cell, Ni–SDC|SDC|LSCF–SDC, LSCF with and without a separate catalyst layer, Ru–CeO_2|PSZ–CeO_2|Ru–CeO_2, tested at 500 °C with 50 sccm 10.7% propane balanced by air in the anode and ambient air in the cathode.

to the leakage current through the ceria electrolyte resulting from the inherent mixed conductivity [17,18]. These low OCV values were unlikely caused by gas leakage through the thin electrolyte or the seal. In fact, the SDC electrolyte was fully dense since the permeability measurement of the as-fired cells yielded a leak rate of $<1.6 \times 10^{-18}$ m^2 that is sufficiently low as a gas-tight layer [1]. Gas leakage through the seal is also minor since the YSZ-electrolyte SOFCs sealed in the same manner gave OCVs only 40–70 mV below the thermodynamically predicted values [8].

The *J–V* curves in Fig. 2a were fairly linear at low current densities, but the resistance increased sharply at high current densities. For comparison, the *J–V* curves in humidified hydrogen fuels were nearly linear over a wide current range, and the presence of a separate catalyst layer had no obvious influence on the cell performance with maximum power densities of ≈1100 mW cm^{-2} at 600 °C and ≈500 mW cm^{-2} at 500 °C as previously reported [17], indicating that the porosities of the PSZ–CeO_2 support and the deposited thin Ru–CeO_2 layers were reasonably high to ensure quick transport of H_2 into, and H_2O out of, the Ni–SDC anode. The limiting current behaviour for propane–air fuel mixtures can be mainly attributed to the relatively dilute hydrogen, typically <20% H_2, produced by the propane partial oxidation reactions [8,9].

Fig. 2b compares electrochemical impedance spectra obtained at open circuits from fuel cells integrated with and without a Ru–CeO_2 catalyst layer. The pure ohmic resistance, corresponding to the high-frequency real-axis intercept (R_o), was nearly unchanged and ≈0.13 Ω cm^2, slightly lower than the calculated value of 0.l8 Ω cm^2 based upon the conductivity of SDC at 500 °C (0.0033 S cm^{-1}) [19] and the thickness of the SDC electrolyte layer in the present fuel cells (6 μm). This difference can be attributed to increased electronic conductivity of SDC electrolytes exposed

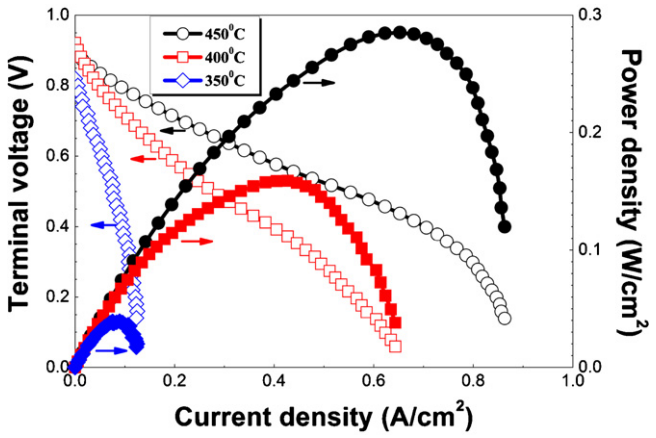

Fig. 3. Voltage and power density vs. current density curves for the cell, Ni–SDC|SDC|LSCF–SDC, LSCF integrated with a separate catalyst layer, Ru–CeO_2|PSZ–CeO_2|Ru–CeO_2, tested with 50 sccm 10.7% propane balanced by air in the anode and ambient air in the cathode at different setpoint temperatures.

to reducing atmosphere in the anode. Notably, integration of a separate catalyst layer as a fuel reformer remarkably reduced the interfacial polarization resistance (R_p) value, 0.46 vs. 0.85 Ω cm^2, as determined from the high and low-frequency real-axis intercepts (denoted as R_o and R_i, respectively). Prior studies suggest that the anodic reaction for internal reforming SOFCs is mainly dominated by electrochemical oxidation of hydrogen produced from the reforming process, specifically from propane partial oxidation in the present studies. Since the cathodic polarization resistance should be about the same for both types of fuel cells with similar cathodes, the large drop in R_p can be explained by the altered anodic behaviour in the presence of the Ru–CeO_2 catalyst layer, exhibiting enhanced partial oxidation of propane and producing higher hydrogen content in the anode chamber.

Fig. 3 shows performance of the fuel cell integrated with a Ru–CeO_2 catalyst layer operating on propane–air fuel mixtures at even lower temperatures. Power densities of practical interest can still be achieved at temperatures as low as 400 °C despite a substantial decrease in the fuel cell performance with decreasing temperature. Maximum power densities measured were 280 mW cm^{-2} at 450 °C and 160 mW cm^{-2} at 400 °C. Further reduction in the operating temperature down to 350 °C resulted in a much lower open circuit voltage value of 0.82 V, opposite to a thermodynamic predicted increase with decreasing temperature, and a smaller maximum power density of 40 mW cm^{-2}, indicative of substantially reduced catalysis of Ru–CeO_2 for propane partial oxidation reactions. Nonetheless, these power densities were comparable to those previously obtained in humidified hydrogen at similar temperatures [12]. In contrast, power densities for the fuel cell without a Ru–CeO_2 catalyst layer, operating on the same propane–air fuel mixtures, dropped to a negligibly small value of <10 mW cm^{-2} for $T \leq 450$ °C. These results suggest that the Ru–CeO_2 catalyst layer is highly effective to promote propane partial oxidation reactions and thereby improve the electrical performance for thin ceria-electrolyte SOFCs, especially at lower temperatures.

Electrochemical oxidation of fuels occurs within an electrochemically active zone in the anode that is 10–20 μm away from the dense electrolyte. Integration of a separate catalyst layer in the fuel cell might alter chemistry and electrochemistry in the anode due to enhanced heterogeneous catalysis as well as increased resistance for transport of fuels toward the catalytically active Ni–SDC layer and for transport of electrochemically formed products such as H_2O and CO_2 away from the electrochemically active zone toward the fuel compartment. Note that the cathodic polarization and

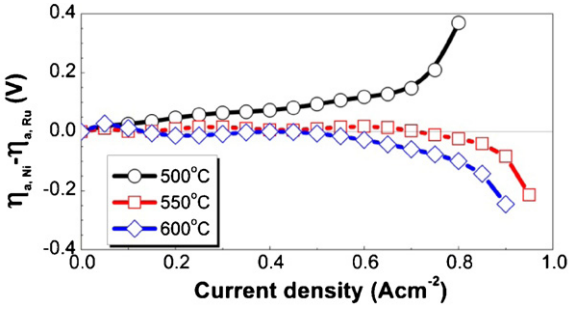

Fig. 4. The anodic overpotential difference vs. current density at different temperatures for the cell operating on propane–air fuel mixtures with and without the Ru–CeO_2 catalyst layer.

the ohmic resistance are both expected to be independent of the fuel produced, with or without an additional catalyst layer, from propane partial oxidation. As suggested by Uda et al. [20], simply comparing the *J–V* curves in Fig. 2a yielded a difference in the anodic polarization for fuel cells integrated with and without a Ru–CeO_2 catalyst layer, *i.e.*, $\Delta\eta_a = \eta_{a,Ni} - \eta_{a,Ru}$, where $\eta_{c,Ru}$ and $\eta_{a,Ni}$ are the anodic polarizations for fuel cells integrated with and without a Ru–CeO_2 catalyst layer, respectively. Fig. 4 shows $\Delta\eta_a$ as a function of current density. Note that results at 550 °C and 600 °C were also included for comparison. The anodic polarization at 500 °C for the fuel cell integrated with a Ru–CeO_2 catalyst layer is smaller than without, *i.e.*, $\eta_{a,Ru} < \eta_{a,Ni}$, consistent with the impedance observations in Fig. 2b. The $\Delta\eta_a$ value increased gradually and became increasingly large for $J > 0.7$ A cm^{-2} when hydrogen was electrochemically oxidized at a higher rate than produced via propane partial oxidation reactions under the catalysis of Ni–SDC anodes. In contrast to the behaviour at 500 °C, the anodic polarizations at 550 °C and 600 °C were nearly the same for $J < 0.5$ A cm^{-2}, and then $\eta_{a,Ru}$ became increasingly larger than $\eta_{a,Ni}$. Note that the anode polarization is related to its electrochemical oxidation and/or the resistance to mass transport. Similar anodic polarizations at low current densities suggested that Ni–SDC anodes provided reasonably high catalytic activity at high temperatures for propane partial oxidation reactions to produce sufficient amount of hydrogen for the subsequent fuel cell operation. On the other hand, larger anodic polarizations at high current densities for the fuel cell integrated with a catalyst layer than without indicates that the catalyst layer increased hydrogen diffusion resistance even though the former had a higher hydrogen content in the reformate than the latter [8,9]. Power output for the fuel cell with a catalyst layer was therefore limited by hydrogen diffusion at high temperatures. For example, maximum power densities of 450 mW cm^{-2} were observed at 550 °C and 600 °C as well, lower than the respective values of 500 mW cm^{-2} and 660 mW cm^{-2} for the fuel cell without a catalyst layer operating on the same fuel mixture of 10.7% propane–89.3% air.

4. Conclusions

In summary, we have demonstrated that thin film catalysts, consisting of nano-scale ruthenium particles well dispersed in the ceria matrix, enabled impressively high power densities of thin ceria-electrolyte SOFCs at low temperatures when directly operating on the propane–air fuel mixtures, *e.g.*, 390 mW cm^{-2}, 280 mW cm^{-2} and 160 mW cm^{-2} at 500, 450 and 400 °C, respectively. The success of the catalyst can be ascribed to its high catalytic activity for propane partial oxidation reactions, producing hydrogen for the fuel cell operation. Such high power densities at low temperatures, combined with high fuel efficiencies and readily availability of propane fuels, would make the integrated design highly attractive for portable and transportation applications.

Acknowledgements

The authors gratefully acknowledge the financial support of the National Science Foundation of China under Contract No. 51072219, Science and Technology Commission of Shanghai Municipality under Contract No. 09JC1415200 and the 100 Talents Program of Chinese Academy of Sciences.

References

[1] P. Von Dollen, S. Barnett, J. Am. Ceram. Soc. 88 (2005) 3361–3368.
[2] A. Atkinson, S. Barnett, R.J. Gorte, J.T.S. Irvine, A.J. Mcevoy, M. Mogensen, S.C. Singhal, J. Vohs, Nat. Mater. 3 (2004) 17–27.
[3] S.D. Park, J.M. Vohs, R.J. Gorte, Nature 404 (2000) 265–267.
[4] Y.H. Huang, R.I. Dass, Z.L. Xing, J.B. Goodenough, Science 312 (2006) 254–257.
[5] S.W. Tao, J.T.S. Irvine, Nat. Mater. 2 (2003) 320–323.
[6] J.M. Haag, B.D. Madsen, S.A. Barnett, K.R. Poeppelmeier, Electrochem. Solid St. 11 (2008) B51–B53.
[7] D.M. Bierschenk, E. Potter-Nelson, C. Hoel, Y.G. Liao, L. Marks, K.R. Poeppelmeier, S.A. Barnett, J. Power Sources 196 (2011) 3089–3094.
[8] Z.L. Zhan, J. Liu, S.A. Barnett, Appl. Catal. A: Gen. 262 (2004) 255–259.
[9] Z.L. Zhan, S.A. Barnett, Solid State Ionics 176 (2005) 871–879.
[10] Z.L. Zhan, S.A. Barnett, Science 308 (2005) 844–847.
[11] N.M. Sammes, R.J. Boersma, G.A. Tompsett, Solid State Ionics 135 (2000) 487–491.
[12] Z.P. Shao, S.M. Haile, Nature 431 (2004) 170–173.
[13] C.S. Ding, T. Hashida, Energ. Environ. Sci. 3 (2010) 1729–1731.
[14] T. Suzuki, T. Yamaguchi, K. Hamamoto, Y. Fujishiro, M. Awano, N. Sammes, Energ. Environ. Sci. 4 (2011) 940–943.
[15] T. Hibino, A. Hashimoto, T. Inoue, J. Tokuno, S. Yoshida, M. Sano, Science 288 (2000) 2031–2033.
[16] Z.P. Shao, S.M. Haile, J. Ahn, P.D. Ronney, Z.L. Zhan, S.A. Barnett, Nature 435 (2005) 795–798.
[17] Z.L. Zhan, S.A. Barnett, J. Power Sources 157 (2006) 422–429.
[18] Z.L. Zhan, S.A. Barnett, J. Power Sources 155 (2006) 353–357.
[19] B.C.H. Steele, Solid State Ionics 129 (2000) 95–110.
[20] T. Uda, D.A. Boysen, C.R.I. Chisholm, S.M. Haile, Electrochem. Solid St. 9 (2006) A261–A264.